ELSEVIER

Journal of Food Engineering 61 (2004) 309–319

JOURNAL OF FOOD ENGINEERING

www.elsevier.com/locate/jfoodeng

A mathematical model of direct sun and solar drying of some fermented dairy products (Kishk)

A.H. Bahnasawy [a,*], M.E. Shenana [b]

[a] Faculty of Agriculture, Department of Agricultural Engineering, Zagazig University, P.O. Box 13736 Moshtohor, Benha Branch, Egypt
[b] Faculty of Agriculture, Moshtohor, Department of Food Science, Zagazig University, Benha Branch, Egypt

Abstract

A *mathematical* model of direct sun and solar drying of some fermented dairy products (Kishk) was developed. Solar radiation, heat convection, heat gained or lost from the dryer bin wall and the latent heat of moisture evaporation were the main components of the equations describing the drying system. The model was able to predict the drying temperatures at a wide range of relative humidity values. It has also the capability to predict the moisture loss from the product at wide ranges of RH values, temperatures and air velocities. The model showed a dramatic effect of the air velocity on increasing the moisture loss at the beginning of the drying process and became constant which leads to a recommend that it is better to use low temperature with forcing air at the beginning of drying. In the next stages, high temperature without forcing air should be used. The model was validated by using experimental data of the drying temperatures and moisture loss under both direct sun and solar drying systems for five fermented dairy products (Kishk). The predicted values were in a reasonable agreement with the experimental data. The coefficients of determination for the predicted moisture loss in case of the sun drying system were lower than those under the solar drying. This may be attributed to the deeper grooves and cracks on the surface of the products, the heat conducted from the drying trays and the variation of the measured wind speed.

Keywords: Fermented dairy products; Drying; Model; Moisture; Kishk

1. Introduction

The removal of water from the foods provides microbiological stability, reduces deteriorative chemical reactions and reduces transportation and storage costs. Most of food dehydration processes take place in the falling rate period, during which water is transported from the interior to the surface by various mechanisms and is usually analyzed by diffusion (Uzman & Sahbaz, 2000).

Drying of agricultural products under direct sunlight is the traditional way of preservation of foods. Traditional sun drying takes place by putting the products under the direct sunlight or indirect by covering the products by transparent or non-transparent covers. In the last method the sun heating is indirect through heating of connective air. Drying with the various forms of solar drying has the advantage of small or negligible installation and energy costs. However, the running costs may be high because of solar drying, being a slow process due to the climatic variation, is a labour intensive operation (Karathanos & Belessiotis, 1997).

Solar drying systems became an important method of drying agricultural products. Solar conversion technologies differ from region to another, because of the variation in the solar intensities and some economical and industrial factors. The solar energy incident on Egyptian land ranges from 5 to 8 kW h/m^2/day (Sayigh, 1977).

The fermented dairy cereal product (Kishk) is a very popular dried food in Middle East and Egypt, especially in Upper Egypt. This product is basically made from a combination of wheat with natural local sour milk (Laban Khad, Laban Zeer or Laban Rayeb). The mixture is shaped then dried in the hot shade or sun. This product is rich in nutritive constituents, and is a possible source of many vitamins and growth factors associated with the microbial fermentative processes (El-Gendy, 1983).

Kishk is a balanced food with an excellent keeping quality, richer in B vitamins than either milk or wheat

* Corresponding author.
E-mail address: bahnasawyadel@hotmail.com (A.H. Bahnasawy).

0260-8774/$ - see front matter © 2003 Published by Elsevier Ltd.
doi:10.1016/S0260-8774(03)00134-1

Nomenclature

A_c	is the surface area of the solar collector (m^2)
a_i	constant
A_o	is the surface area of the product (m^2)
A_w	is the drying cover surface area (m^2)
c_p	specific heat of air (1.005 kJ/kg °C)
C_t	is the overall mass transfer coefficient (kg/s m^2 kPa)
D	the diffusivity of water vapor of air (m^2/s)
d_p	is the product balls diameter (m)
E	is the emission from the cover surface to the environment $= \delta T_s^4$
h_c	is the connective heat transfer coefficient (W/m^2 °C) $= Nu\,k_a/d_p$
H_s	is the hourly solar radiation on the horizontal surface (W/m^2)
H_{sky}	is the emission from the sky $= \delta T_{sky}^4$
k_a	thermal conductivity of air (0.024 W/m K)
k_{ca}	is the air film mass transfer coefficient (kg/s m^2 kPa)
k_t	is the skin mass transfer coefficient (kg/s m^2 kPa)
k_w	is the thermal conductivity of the drying wall (0.78 W/m K for the glass)
L_c	is the thickness of the glass (0.03 m)
M_a	is the flow rate of drying air
m_{eq}	is the equilibrium moisture content
m_f	is the final moisture content
m_i	is the initial moisture content
M_{loss}	is the moisture loss rate from the product (kg/s)
m_p	is the mass product ball (kg)
MR	is the moisture ratio
m_t	is the average moisture content at a certain time (%, wb),
Nu	is Nusselt number (–) $= 2.0 + 0.552(Re)^{0.53} \times (Pr)^{0.33}$
P_{amb}	is the water vapor pressure of the surrounding air (kPa)
Pr	Prandtl number (–) $= \mu * c_p/k$
P_s	is the water vapor pressure of the evaporating surface (kPa)
Q_{conv}	is the heat transferred by convection from the surface to environment (W/m^2), $Q_{conv} = h_c(T_s - T_{amb})$
Q_e	is the heat for evaporation moisture from the product (W)
Q_l	is the latent heat of water evaporation (2445.2 kJ/kg) at 25 °C and 1 atmosphere pressure
Q_p	is the heat gained by product (W)
Q_s	is the net solar heat transmitted to the drying cover surface (W)
Q_w	is the heat transferred through the drying wall (W)
Re	Reynolds number (–) $= \rho v d_p/\mu$
RH	is the relative humidity (%)
Sc	Schmidt number (–) $= \mu/\rho D$
Sh	is Sherwood number (–) $= 2.0 + 0.552 \times (Re)^{0.53}(Sc)^{0.33}$
T_{amb}	is the ambient temperature (K)
T_{in}	is the temperature inside the drying bin (K)
T_s	is the sun collector surface temperature (K)
v	is the air velocity (m/s)
VPD	is the water vapor pressure deficit (kPa)
W_1	is the moisture of the incoming drying air
W_2	is the moisture of the outgoing drying air
α	is the average absorptivity of the cover (0.98) for painted black body
δ	is Stefan–Boltzmann constant $= 5.669 \times 10^{-8}$ (W/m^2 K^4)
T_{sky}	is the sky temperature (K), $T_{sky} = 0.0552 T_{amb}^{1.5}$
ρ	is the air density (1.2 kg/m^3)
μ	is the air viscosity (1.7×10^{-5} N s/m^2)
α_s	is the absorptivity of the cover surface (0.9)
α_{sky}	is the emissivity of the sky (0.1)

and well adapted to hot climates by its content of lactic acid. It probably has a therapeutic value similar to yoghurt (Abd El-Malek, 1978). Dried Kishk is not hygroscopic and can be stored in an open jar for two or three years without deterioration (Abou-Donia, Attia, Khattab, & El-Shenawi, 1991; Tamime & O'conner, 1995; VanVeen, Graham, & Steinkraus, 1969).

Several mathematical models on solar drying have been developed by many researchers (Phoungchandang & Woods, 2000; Sabbah, Keener, & Meyer, 1979).

Conceptualization of drying involves the single particle alone and the particles in mass, and many of drying models have been developed for both cases. When drying a single particle (or thin layer-drying), the empirically fitted curves as well as the theoretical curves based on heat and mass transfer for rate of moisture loss take the following form (Hansen, Keener, & El-Sohly, 1993):

$$\mathrm{MR} = \frac{m_t - m_i}{m_{eq} - m_i} = \sum_{n=1}^{\infty} a_i e^{-kt} \tag{1}$$

However, Weller and Bunn (1993) used the weight change over time to calculate the moisture change over the time. A drying rate constant (k) was derived by fitting moisture content and time to a thin-layer drying equation of the form:

$$\mathrm{MR} = \frac{m_t - m_f}{m_i - m_f} = e^{-kt} \quad (2)$$

Final moisture content was used in the equation as opposed to an equilibrium moisture such as suggested by Brooker, Bakker-Arkema, and Hall (1974) since a final moisture content is more realistic from a practical standpoint.

The purpose of this study was to: (1) predict temperature inside the dryer at different relative humidity values and ambient temperatures, (2) predict the moisture loss from the products at different RH, temperatures and air velocities and (3) validate the model with the experimental data.

2. Model development

Heat and mass balances were carried out in order to describe the drying system. The temperature rise and moisture loss during the drying are described by means of the transient energy conservation equation, combined with an equation for the rate of moisture loss. However, the following assumptions were made in developing the model:

1. The product is uniformity distributed in the drying space.
2. Product balls are characterized as homogenous objects and have a uniform temperature.
3. A steady state condition is achieved.
4. The coefficient of evaporation remains constant.

2.1. Heat balance

The heat balance equation is based on the concept that the algebraic summation of the rate of sensible energy gain, the absorbed solar heat, heat gain or heat loss from the dryer wall, and the heat loss due to the moisture evaporation. These could be explained as follows:

1. Heat absorbed from the solar radiation,
2. Heat gained or lost by the product,
3. Heat gained or lost through the drying bin wall, and
4. The latent heat of the moisture evaporation from the product.

These components can be written as follows:

$$Q_s \pm Q_p \pm Q_w - Q_e = 0 \quad (3)$$

With reference to Fig. 1, the values of Q_s, Q_p, Q_w and Q_e can be calculated from the following equations:

$$Q_s = \alpha_s H_s + \alpha_{sky} H_{sky} - Q_{conv} - E \quad (4)$$

$$Q_p = m_p c_p (T_{in} - T_{amb}) \quad (5)$$

$$Q_w = k_w A_w (T_{in} - T_{amb})/L_c \quad (6)$$

$$Q_e = A_o C_t (P_s - P_{amb}) * Q_l \quad (7)$$

Substituting equations from (4)–(7) and re-arranging yields the following equation:

$$T_{in} = \frac{A_o C_t (P_s - P_{amb}) Q_l - 0.9 H_s + 10^{-12} T_{amb}^{1.5} + h_c A_c (T_s + T_{amb}) + m_p c_p T_{amb} + k_w A_w T_{amb}}{m_p c_p + k_w A_w / 0.03} \quad (8)$$

2.2. Mass balance

At the moisture balance, moisture losses are equal to the moisture sources. Moisture sources are the water evaporation from the product and moisture incoming with the drying air. Moisture losses are the losses outgoing with the drying air and the moisture losses from the air by condensation. A simple of the moisture balance can be written as follows (Midwest Plane Service, 1980):

$$M_a (W_2 - W_1) = M_{loss} \quad (9)$$

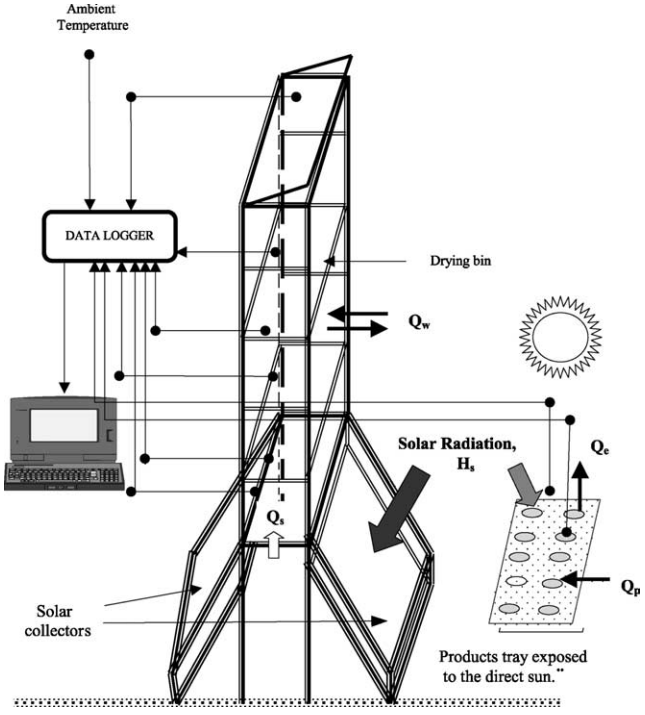

Fig. 1. Schematic diagram showing solar drier, the products on the tray for direct sun drying and the main components of the heat and mass balance.

In practical, the heat transfer equation gives a better estimate of the drying rate than the mass transfer equation.

The mass transfer coefficient is not only a function of the product skin resistance but also it is related to the resistance to molecular diffusion of water vapor from the product surface to the free air stream as discussed by Fockes and Meffert (1972). Hence, the rate of the moisture loss will be:

$$M_{\text{loss}} = \frac{A_{\text{o}}(\text{VPD})}{1/k_{\text{ca}} + 1/k_{\text{t}}} \tag{10}$$

The coefficient of determination (R^2) of this equation was 0.992. Skin mass transfer coefficient is dependent upon the structure and properties of the product surface, however, the air film coefficient is dependent upon the size of product as well as the properties of flow rate of the surrounding air. The film mass transfer coefficient (k_{ca}) can be calculated from the Sherwood–Reynolds–Schmidt correlation

$$Sh = k_{\text{ca}} * d_{\text{p}}/D \tag{11}$$

2.3. Water vapor pressure deficit (VPD)

The water vapor pressure deficit is the difference between the vapor pressure of the intercellular spaces in the product and the vapor pressure of the surrounding air. Vapor pressure deficit can be calculated using the following equation (Misener & Shove, 1976):

$$\text{VPD} = P_{\text{s}}(1.00 - \text{RH}) \tag{12}$$

The vapor pressure deficit is a function of both temperature and relative humidity. The following form is the best relationship between the VPD, temperature and relative humidity with a coefficient of determination of 0.99 (Bahnasawy, 1999):

$$\text{VPD} = 0.293 + 0.0741T + 0.0029\text{RH} - 0.0015T * \text{RH} + 0.0019T^2 \tag{13}$$

2.3.1. Weather data

Ambient atmospheric conditions such as dry-bulb temperature, relative humidity, solar radiation and wind velocity are the primary component of many mathematical models in agriculture. These data can be obtained, usually with considerable difficulty, from the historical climatic records. Climatic records, however, are often incomplete and difficult to manipulate and incorporate into a model. Simulation can be used as an alternative source of climatic data, which is more compact and readily available than historic records. Fourier analysis was used as a deterministic model to simulate these parameters. The simulation was carried out during the months of June to August in Cairo, Egypt.

Table 1
Fourier coefficients for various weather data parameters for the months of June–August for Cairo, Egypt

Fourier coefficients	Weather parameters			
	Temperature (°C)	RH (%)	Solar radiation (MJ/m^2 h)	Wind velocity (m/s)
a_0	51.65	159.70	2.18	5.79
a_1	−6.28	18.42	−1.57	3.17
b_1	−2.16	2.89	0.65	−1.04
a_2	1.76	−6.53	0.49	−0.64
b_2	−0.212	−1.98	−0.50	0.41
a_3	0.237	1.48	−0.02	−0.28
b_3	0.267	0.79	−0.03	−0.21
a_4	−0.283	−0.62	0.01	0.08
b_4	0.08	0.14	0.11	0.25
a_5	−0.08	0.56	0.01	−0.14
b_5	−0.07	0.29	0.05	−0.16
a_6	0.13	0.52	−0.07	0.13
b_6	−0.04	−0.34	−0.08	0.19

$$\begin{aligned} f(t) &= \frac{a_{\text{o}}}{2} + \sum_{n=1}^{\infty}(a_n \cos n\omega t + b_n \sin n\omega t) \\ &= \frac{a_{\text{o}}}{2} + a_1 \cos n\omega t + a_2 \cos n\omega t + \cdots \\ &\quad + b_1 \sin n\omega t + b_2 \sin n\omega t + \cdots \end{aligned} \tag{14}$$

where $f(t)$ represents the temperature, relative humidity, solar radiation and wind velocity; $n = 0, 1, 2, \ldots, 2N$; $\omega = 2\Pi/L$; $L = 2N + 1$, $N = 12$ h; t is the day hours (1:00 am = hour # 1); a_{o}, a_1, a_2, b_1, and b_2, ... are the Fourier coefficients as shown in Table 1.

These coefficients can be calculated as follows (Ralston & Wilf, 1960):

$$a_n = \frac{2}{2N+1} \sum_{n=0}^{2N} f_{\text{t}} \cos \frac{2\pi np}{2N+1} \tag{15}$$

$$b_n = \frac{2}{2N+1} \sum_{n=1}^{2N} f_{\text{t}} \sin \frac{2\pi np}{2N+1} \tag{16}$$

2.4. Computer program

A Fortran program was used to simulate the heat and mass balance for the drying system, the required weather data generation and the thermal and physical properties of the product and the air. The heat and mass balance (Eqs. (3)–(16)) were solved.

The program was written using Fortran-77 programming language. The computer program consisted of one main program. The main program was divided into three parts in addition to the input parts. *The first* part was devoted to simulate the weather data required to be generated into the main program. *The second* part was devoted to predict the drying temperature at different RH values. *Finally, the third* part was used to predict the moisture loss from the products under different temperatures, RH values and air velocities.

3. Experimental procedures

Low-heat skimmed milk powder (made in Holland) was obtained from the local Egyptian market. Dried wheat was obtained from the Kalubia Governorate market, Soy products (whole Soy flour, deffated Soy flour and Soy bran) were obtained from Food Technology Research Institute, Agriculture Research Center (ARC), Giza, Egypt. Mung bean was obtained from Agriculture Research Center, Faculty of Agriculture, Moshtohor, Benha Branch, Zagazig University, Egypt.

A commercial yoghurt starter culture containing *Streptococcus salivarius* sub spp *thermophilus* and *Lactobacillus delbrueckii* sub spp *bulgaricus* was used in making the fermented skimmed milk. Commercial fine grade salt was used. Fermented dairy cereal products (Kishk) were made by the methodology as described by Shenana, Bahnasawy, and El-Desouky (2001) as follows:

First fermentation: Skimmed milk was reconstituted at a rate of ~10% total solids (TS), activated starter culture was added at a rate of 2% and incubated at 40 °C until the pH reached 4.6. Four parts of fermented skimmed milk was mixed with one part of parboiled wheat, Mung bean, whole soy bean flour, deffated soy flour, or soy bran to form P1, P2, P3, P4 and P5 (w/w), respectively.

Second fermentation: The mixed products were held at 40 °C for three days with daily agitation and the products were kept under sanitation conditions. After that, the salt was added at rate of ~1% to reduce the starter culture activity. The products were shaped into small, round pieces (balls) and placed on perforated metal trays.

The solar drier consists of main drying chamber and two plates as solar collectors. The length, width and height of the frame (Fig. 1) are 0.6, 1.0, and 1.65 m, respectively. The solar collectors are made from a black sheet as an absorber plate (1.0×1.0 m) and covered with a single glass (3.0 mm thickness). The distance between the glass cover and the black plate is 12.0 cm. These collectors are placed one on the east side of the chamber and the other one on the west side.

Data logger was used to launch the temperature data from nine sensors at different locations and times of the day as shown in Fig. 1. These sensors were distributed as follows: one at the end of solar collector, one at the exhaust opening of the drier, four at the dryer shelves, one at the ambient and two at the trays of the direct sun drying system.

Thermohydrometer (Sigma II Model NSIIQ, type no. 7210.00, SK SATO-KEIRYOKI mfg. Co., LTM, Tokyo, Japan) was used to record the RH in the drying bin as well as at the ambient RH of the air surrounding the bin.

The wind speed at the location of the drying was measured by using (Vane Thermo-anemometer, 0.7, LCD/3-1/2 digits, measure range is 0.4–30 m/s, Extech Instruments).

During the drying time, samples of the products were taken to determine the changes in moisture content using Infra-red moisture determination balance (Kett Electrical Product Laboratory FD-620, Japan). This work has been done during the period of June–August, 2001.

3.1. Some thermal and physical properties of the fresh products (Kishk)

The specific heat, surface area, weight, volume and density of the fermented dairy cereal products (Kishk) involved in this model as inputs were determined and listed in Tables 2 and 3. The simplest form of the equation for estimation the approximate specific heat c_p of food is as follows:

$$c_p = m_w c_w + m_s c_s \ (\mathrm{kJ/kg\,K}) \tag{17}$$

where m_w is the mass fraction of water, $c_w = 4.18$ kJ/kg K is the specific heat of water, m_s is the mass friction of solids and $c_s = 1.46$ kJ/ kg K (Lamb, 1976) is the specific heat of solids. This reflects the major contribution due to water content using Eq. (17), the c_p of the products were estimated from both the water and total solids contents.

The products were dried using two methods: *first*, sun drying where the trays were placed on the direct sun radiation. *Second* was the solar drying, where the

Table 2
The specific heat of the fresh fermented dairy cereal products (Kishk)

Product	c_p (kJ/kg K)		Total
	m_w	m_s	
P1	2.250	0.370	2.620
P2	1.550	0.310	1.860
P3	1.670	0.290	1.960
P4	1.660	0.220	1.880
P5	1.430	0.257	1.687

P1: product made from parboiled wheat, P2: Mung bean, P3: whole soybean flour, P4: deffated soy flour and P5 is the product made from soy bran.

Table 3
Some physical properties of the fresh fermented dairy cereal products (Kishk)/ball

Product	Character			
	Surface area (m^2)	Weight × 10^{-3} (kg)	Volume × 10^{-6} (m^3)	Density × 10^{-3} (kg/m^3)
P1	0.065	79.36	75.00	1.053
P2	0.052	58.00	65.00	0.892
P3	0.056	59.68	55.00	1.085
P4	0.037	55.06	55.00	1.001
P5	0.034	51.85	55.00	0.943

product's trays were put on the shelves of the drying bin and the hot air was passing through these trays upward from the solar collectors. Drying time and final moisture content for each product were recorded. Also, the trays were shifted alternatively inside the solar bin in order to give the same chance for the products to have the same drying conditions.

4. Results and discussion

4.1. Model sensitivity

Before the model is validated against the experimental data, it was useful to test the sensitivity of model to the changes of the ambient RH values on the predicted drying temperature. The changes of different temperatures, RH values and air velocities inputs on the predicted moisture loss from the products under solar drying system were also determined.

4.1.1. Effect of the ambient RH values at ambient temperature on the predicted temperature inside the drying bin

Fig. 2 shows the predicted temperature inside the drying bin at different relative humidity values (20–100%) under the ambient temperature and a wind speed of 0 m/s during 24 h day. It is clear that inside the drying bin the temperature increased with the decrease of the relative humidity. Temperature inside the drying bin was higher by 3–7 °C than the ambient temperature at the peak of the curve (10:00 am–6:00 pm) at the lowest RH levels (20%). However, the highest variations were observed at the range of 20–60% of RH, on the other hand, there were slight differences at the range of 80–100% RH. It means that the model has low sensitivity to the changes of RH values above 80%.

4.1.2. Effect of different temperatures and RH values on the moisture losses from the products

Fig. 3 shows the predicted moisture loss of the products P1, P2, P3, P4 and P5, respectively, which, dried under different temperatures (20–50 °C), RH values ranged from (40–100%) and air velocity of 0 m/s as is taken place in the solar drying bin. The model demonstrated that, the moisture loss from the products increased with the increase of drying temperature under all RH values for all the products. On the other hand, the predicted moisture loss decreased with increasing of relative humidity and this was mainly due to decrease of the water vapor pressure deficit as the main reason of moisture evaporation (Toledo, 1991).

The model was able to predict the moisture loss at low temperature and high RH, which gave negative values of moisture loss. This means that the products under these conditions start to absorb the moisture from ambient conditions, which leads to an increase in the moisture content of the products.

4.1.3. Effect of different air velocities and RH values on the moisture losses from the products

In order to assess the possibility of forcing air with different velocities during the drying process, different air velocities were input to model at different RH values and at a certain temperature.

Fig. 4 shows the predicted moisture loss from P1, P2, P3, P4, and P5 at different values of RH (40–100%) and air velocities (0–5.0 m/s). The model showed that, there is a dramatic effect of the air velocity on moisture loss under different values of RH. The model demonstrates that the moisture loss increased rapidly with the increase of air velocity at the beginning of drying and slowed down until it became approximately constant even with the increase of the air velocity. This leads us to conclude that the low temperature and high air velocity can be

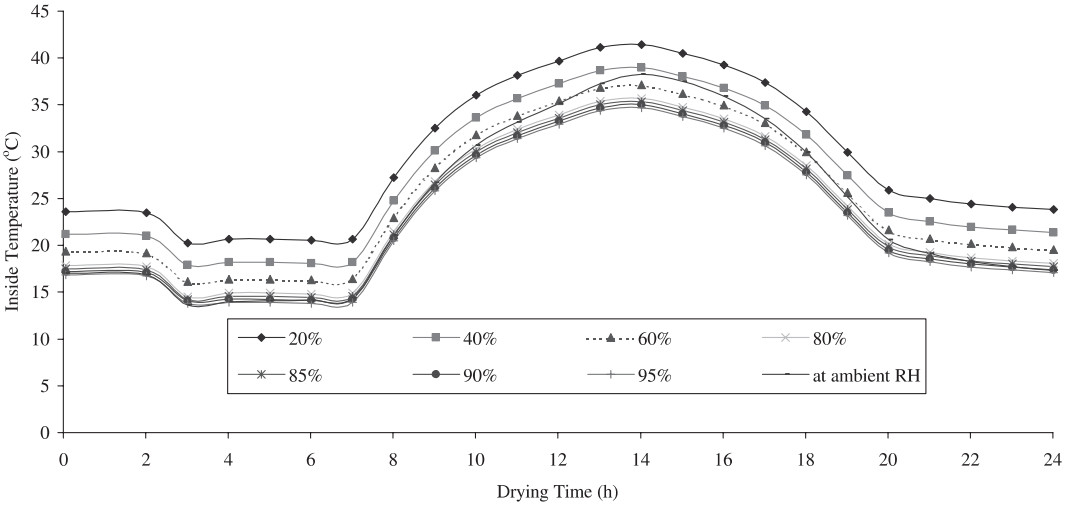

Fig. 2. Predicted temperature inside the drying bin as influenced by the ambient temperature and different RH values.

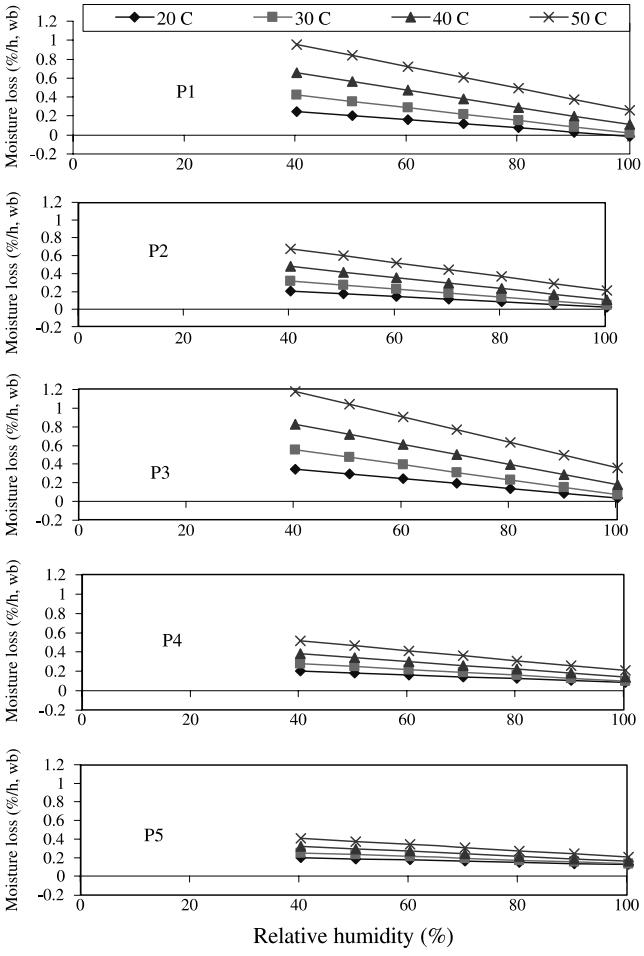

Fig. 3. The predicted moisture loss as influenced by temperature and relative humidity for different products.

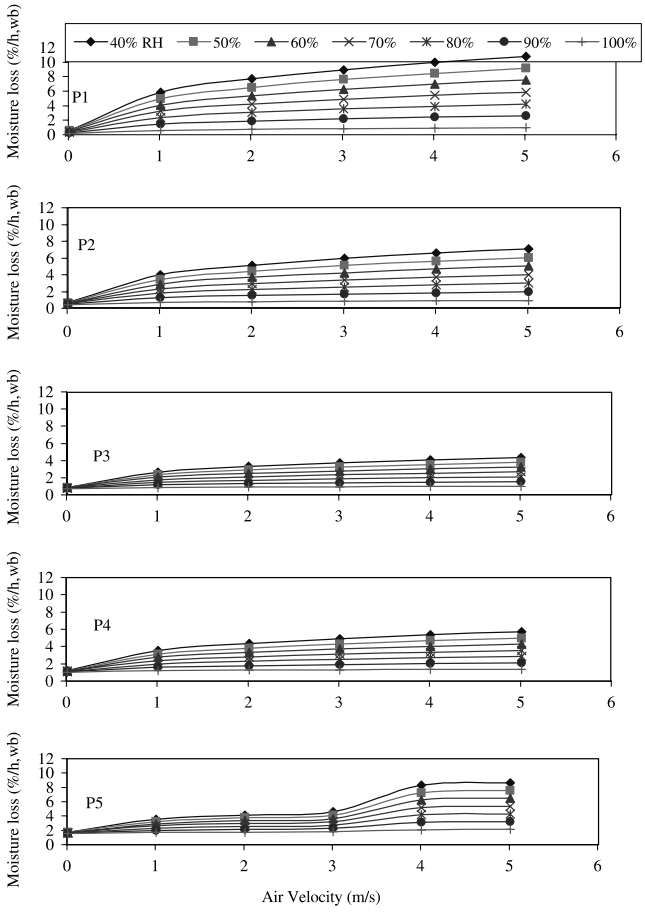

Fig. 4. The predicted moisture loss as influenced by air velocity and relative humidity for different products at 35 °C ambient temperature.

used at the beginning of drying and high temperature with lower air velocity at the next stage, similar observations were reported by Karathanos and Belessiotis (1997). Also, from the obtained results it can be seen that the moisture loss increased with the decrease of RH values at the same temperature and air velocity.

4.2. Model validation

The reliability of the moisture loss obtained with the model can be determined by comparison with the experimental results. For comparison purposes, the coefficient of determination and the average relative percentage of the prediction errors were estimated. The average relative percentage of prediction error (ARPPE) was estimated by using the following form:

$$\text{ARPPE} = \text{Average}\frac{\text{Predicted value} - \text{Experimental value}}{\text{Experimental value}} \quad (18)$$

4.2.1. Drying temperature

Fig. 5 shows the comparison between the predicted and measured drying temperatures for both the solar and direct sun drying systems. It shows that there was a good agreement between the measured and predicted values with coefficient of determination (R^2) of 0.903

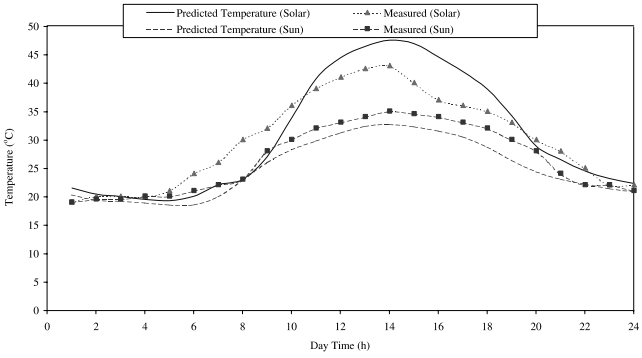

Fig. 5. The predicted and measured temperatures inside the solar bin and ambient for sun drying system.

and 0.97 for solar and sun drying systems, respectively. The average relative percentages of prediction errors were 0.873 + 11.5 and −5.21 + 4.58% in the same pervious order. It is also indicated that the predicted temperature at sun drying system was lower than the measured temperature. The explanation for this may be due to the cooling effect of the wind speed in reducing the temperature around the products in the sun drying system (Phoungchandang & Woods, 2000).

4.2.2. Moisture loss

Figs. 6 and 7 show comparison between the predicted and the experimental moisture losses with the drying time for five fermented dairy products (P1, P2, P3, P4 and P5) under solar and sun drying systems. From these results it can be seen that the predicted values are in a reasonable agreement with the experimental results.

For P1, the predicted values were in a good agreement with the experimental with coefficient of determination

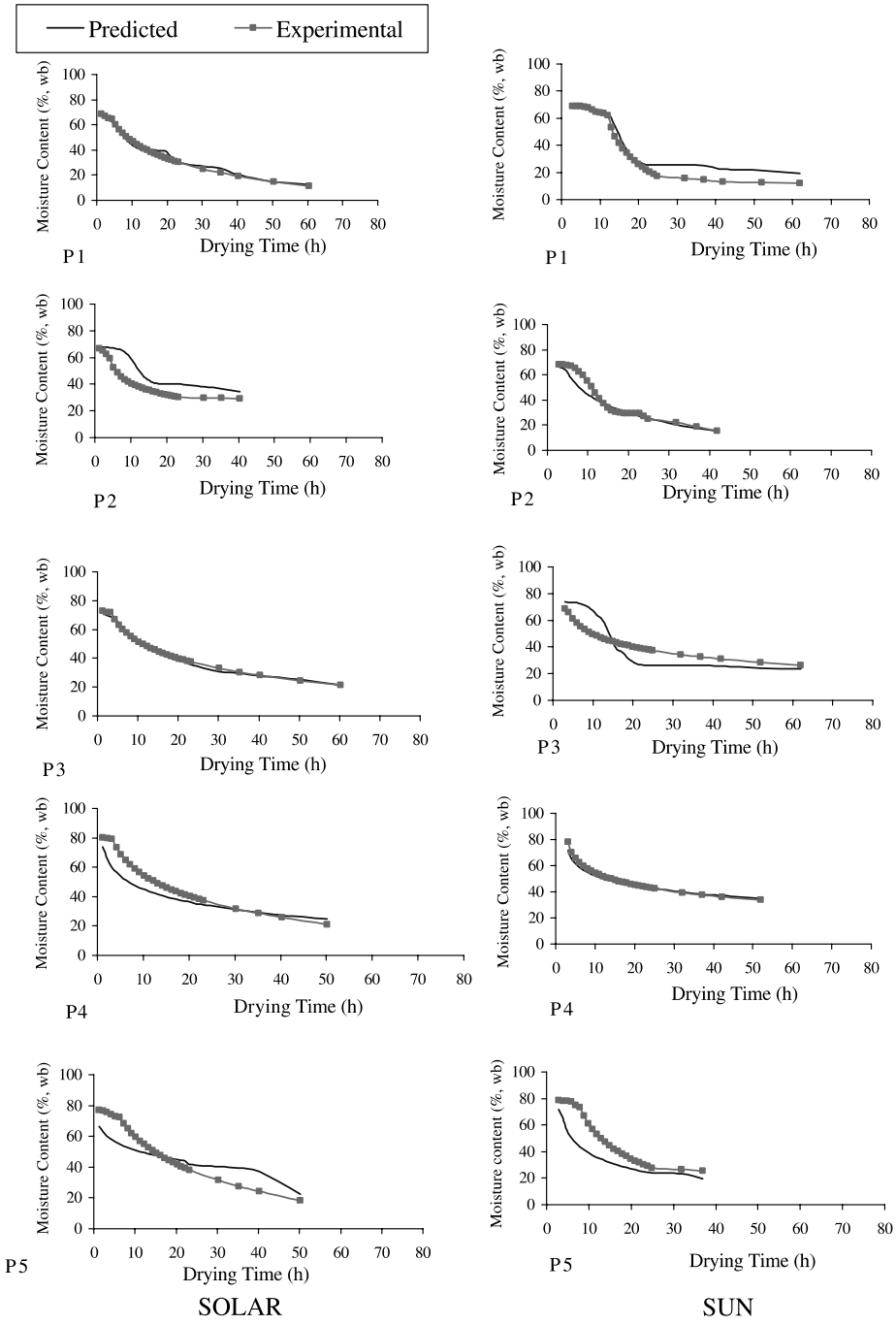

Fig. 6. Predicted and experimental moisture content changes of different products during sun and solar drying.

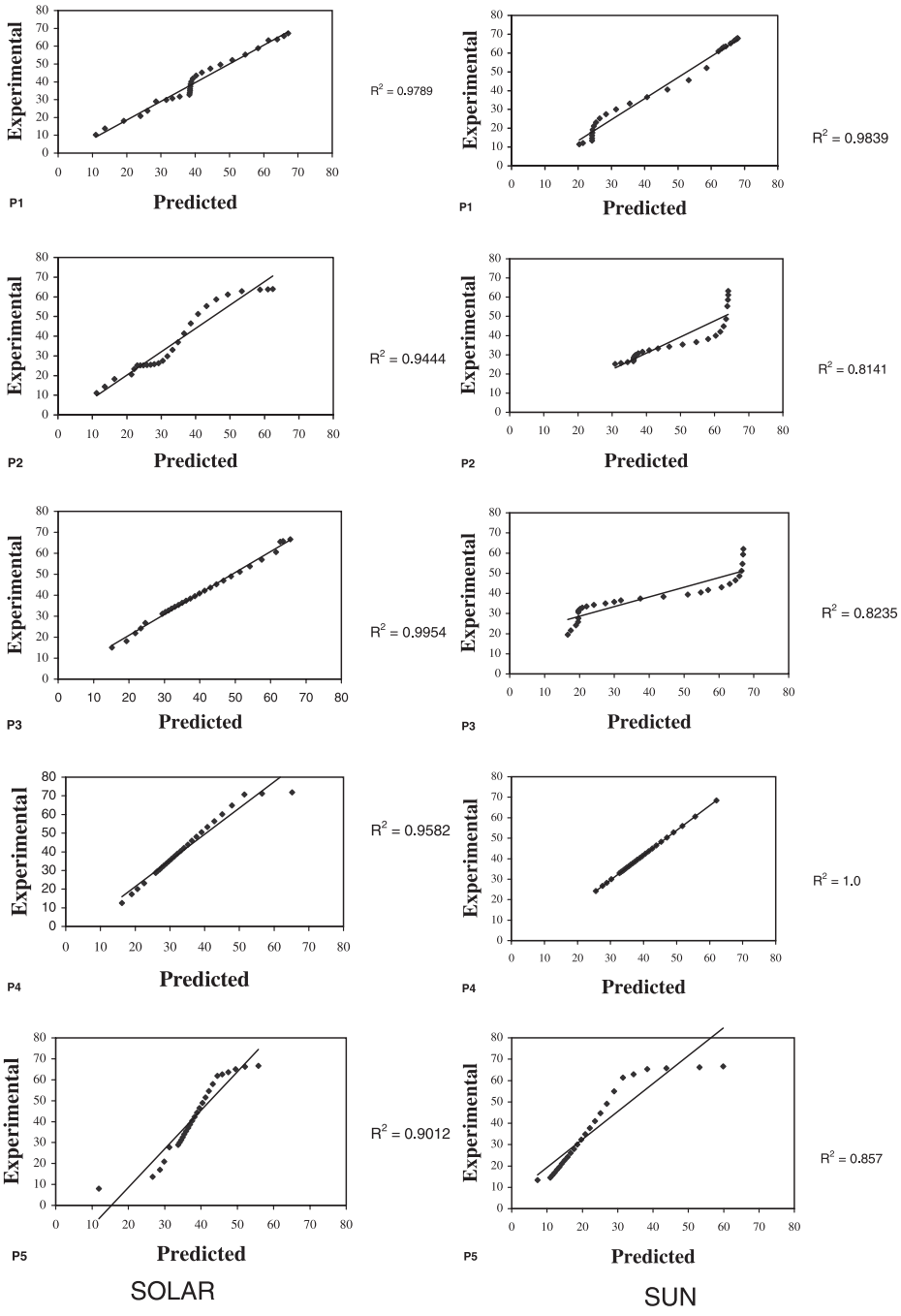

Fig. 7. The coefficient of determination for the predicted and the experimental moisture losses from the products dried under direct sun and solar drying systems.

(R^2) of 0.98 under both solar and sun drying systems, meanwhile, the ARPPE values were $2.64 \pm 7.11\%$ and $21.32 \pm 27.86\%$ for solar and sun drying, respectively. The ARPPE of the sun drying is higher than that of solar drying, this may be due to the variation of the recorded wind speed during the day which, affects the experimental results of the moisture losses under direct sun drying system.

For P2, the coefficients of determination R^2 were 0.94 and 0.814 for the predicted and experimental results in both solar and sun drying, respectively. The ARPPE values were $5.02 \pm 10.02\%$ and $29.54 \pm 13.20\%$ for the same pervious order. Also, the ARPPE of the sun drying was higher than that of solar, this may be due to the effect of air velocity, heat conduction from the trays during drying and the deeper grooves and cracks in the product dried under sun which, caused more moisture evaporation.

Looking at the R^2 values for P3, they were found to be 0.995 and 0.824 for the predicted and experimental

results for both solar and sun drying systems, respectively. The ARPPE values were $2.08 \pm 2.82\%$ and $2.82 \pm 29.54\%$ for solar and sun drying, respectively. It can be noticed that the ARPPE values for the solar and sun drying were similar, but the standard deviation was higher under the sun drying condition for the previous reasons.

In case of P4, the R^2 values were 0.96 and 1.00 and the ARPPE were $13.9 \pm 12.10\%$ and $3.02 \pm 3.46\%$ for solar and sun drying systems, respectively.

On the other hand, R^2 for P5, recorded 0.90 and 0.857 however, the ARPPE values were $1.70 \pm 30.71\%$ and $-35.76 \pm 9.23\%$ for solar and sun drying system, respectively.

In general, the model was able to predict the moisture loss from the five products under two systems of drying (solar and sun) with a reasonable accuracy and the following observations could be made:

1. During the direct sun drying process, some of grooves and cracks were taken place on the drying surface which, increased the moisture evaporation. This may be attributed to that the cracks and grooves acted like fins and the surface area was increased and consequently the heat transfer increased (Mahmutoglu, Pala, & Unal, 1995).

2. Most of the predicted results were lower than that of the experimental ones especially under the direct sun drying system. A reason of this may be owing to the heat transfer coefficient, which may be constant only within the period of a constant rate, while it changes during the falling rate period (Kuts & Pikus, 1980). Also, to the effect of heat conducted from the drying trays, which is not considered in the development of the model.

3. In spite of the low temperature recorded or predicted at the sun drying system compared to solar drying temperature, moisture loss at the same drying time were having no significant differences. This could be attributed to two reasons: *first*, is the effect of wind speed on the increase of moisture loss especially at the beginning of drying process. *Second* is the effect of wind speed in dissipating the water vapor accumulated around the product, which creates a big vapor pressure deficit in the surrounding air of the product, which were not taken place in the solar drying bin.

5. Conclusion

From the experimental and model results, the following points could be concluded:

1. The model was able to predict the temperature of drying at different relative humidity values (RH) and ambient temperature.
2. The model also tested the effect of different RH, temperature and air velocities on the moisture loss.
3. The model was able to predict the temperature under both solar and sun drying systems with coefficient of determination of 0.903 and 0.97, respectively.
4. The model demonstrated that at low temperature and high RH, there was no moisture loss but there was absorption of the moisture by the products.
5. The model results were in a reasonable agreement with the experimental results under both sun and solar drying systems.
6. There were no significant differences between the moisture loss under sun and solar drying systems, this was may be due to the following reasons:
   (a) There were some grooves and cracks that took place on the drying surface in case of the direct sun drying which were much more and deeper than those of solar drying. These grooves and cracks increased the surface area, heat transfer and consequently moisture evaporation.
   (b) The sun trays gained more heat at the sun, which transferred by conduction to the products and increased their temperatures, then moisture loss.
   (c) The effect of wind speed which reached more than 4 m/s in the moisture evaporation especially at the beginning of drying and dissipation the moisture accumulation around the products and in turn, increasing the vapor pressure deficit as the main factor of moisture evaporation in spite of the cooling effect of the air movement.
7. The ARPPE of the model results of temperature and moisture loss under sun drying were higher than those of the solar drying system. This was may be due to the variation of the wind speed during the day, the presence of the grooves and cracks and the heat conducted by the trays, which were not considered in developing the model.

Finally, this model could be used as a tool with the advantages of simplicity and practical accuracy in the design and management of the direct sun and solar drying systems. Also, it is applicable to the heated air or normal air-drying systems in a single layer and sufficiently adaptable to examine the effect of different materials, geometries, air velocities and climates.

References

Abd El-Malek, Y. (1978). Traditional Egyptian dairy fermentation. In W. R. Stanton, & E. J. Dasilva (Eds.), *Glam V. Global impacts of applied microbiology. State of the art: Glam and its relevance to developing countries* (pp. 198–208). KualaLampur, Malaysia: University of Malaya press.

Abou-Donia, S. A., Attia, I. A., Khattab, A. A., & El-Shenawi, Z. (1991). Formulation of dried cereal fermented milks with prolonged storage life. *Egyptian Journal. Dairy Science, 19*(2), 283–299.

Bahnasawy, A. H. (1999). Effect of handling and storage techniques on the quality of some agricultural products. Unpublished Ph.D. Thesis, Agricultural Engineering Department, Faculty of Agriculture, Moshtohor, Zagazig University, Benha Branch.

Brooker, D. B., Bakker-Arkema, F. W., & Hall, C. W. (1974). Theory and simulation of cereal grain drying. *Drying cereal grains* (pp. 185–221). Westport, CT: The AVI Publishing Co.

El-Gendy, S. M. (1983). Fermented foods of Egypt and the middle east. *Journal of Food Protection, 46*(4), 358–367.

Fockes, F. H., & Meffert, H. F. (1972). Biophysical properties of horticultural products as related to loss of the moisture to during cooling down. *Journal of Science, Food Agriculture, 23*, 283–298.

Hansen, R. C., Keener, H. M., & El-Sohly, H. N. (1993). Thin-layer of cultivated taxus clippings. *American Society of Agriculture Engineers, 36*(6), 1873–1877.

Karathanos, V. T., & Belessiotis, V. G. (1997). Sun and artificial air drying kinetics of some agriculture products. *Journal of Food Engineering, 31*, 35–46.

Kuts, P. S., & Pikus, I. F. (1980). Interdependence between heat and mass transfer in drying. In A. S. Mujumdar (Ed.), *Proceedings of the second international symposium—Drying 80: vol. 2* (pp. 65–79). USA: Hemisphere Pauline crop.

Lamb, J. (1976). Influence of water on physical properties of foods. *Chemical Industries, 24*, 1046.

Mahmutoglu, T., Pala, M., & Unal, M. (1995). Mathematical modelling of moisture, volume and temperature changes during drying of pretreated apricots. *Journal of Food Processing and Preservation, 19*, 467–490.

Midwest Plane Service (1980). *Structure and Environment Handbook* (pp. 186–194). Iowa State University, Ames, Iowa 50011.

Misener, G. C., & Shove, G. C. (1976). Moisture loss from kennebec tubers during initial storage period. *Transactions of ASAE*, 967–969.

Phoungchandang, S., & Woods, J. L. (2000). Solar drying of bananas: Mathematical model, laboratory simulation, and field data compared. *Journal of Food Science, 65*, 990–996.

Ralston, A., Wilf, H. S. 1960. Mathematical Methods for Digital computers. V1. New York, London, John Wiley and Sons, Inc., p. 258.

Sabbah, M. A., Keener, H. M., & Meyer, G. E. (1979). Simulation of solar drying of shelled corn using the logarithmic model. *American Society of Agriculture Engineers, 22*(3), 637–643.

Sayigh, A. A. M. (1977). *Solar energy engineering* (first ed.). NY: Academic Press.

Shenana, M. E., Bahnasawy, A. H., & El-Desouky, A. I. (2001). Production of new fermented dairy cereal products (kishk) with different drying methods. *Annals of Agricultural Science, Moshtohor, 39*(4), 2269–2279.

Tamime, A. Y., & O'conner, T. P. (1995). Kishk a dried fermented milk cereal mixture. *International Dairy Journal, 5*, 109–128.

Toledo, T. R. (1991). *Fundamental of food process engineering* (Second ed.). New York: Chapman and Hall, p. 456.

Uzman, D., & Sahbaz, F. (2000). Drying kinetics of hydrated and gelatinized corn starches in the presence of sucrose and sodium chloride. *Journal of Food Science, 65*, 115–122.

VanVeen, A. G., Graham, D. C. W., & Steinkraus, K. H. (1969). Fermented milks wheat combinations. *Tropical and Geographical Medicine, 21*, 47–52.

Weller, C. L., & Bunn, J. M. (1993). Drying rate constants for yellow dent corn as affected by fatty acid ester treatments. *American Society of Agriculture Engineers, 36*(6), 1815–1819.